Hindawi
Journal of Chemistry
Volume 2019, Article ID 9392571, 11 pages
https://doi.org/10.1155/2019/9392571

Research Article

About the Influence of Doping Approach on the Alkali Metal Catalyzed Slow Pyrolysis of Xylan

Valentina Gargiulo, Paola Giudicianni, Michela Alfè, and Raffaele Ragucci

Institute for Research on Combustion (IRC-CNR), P.le V. Tecchio 80, 80125 Naples, Italy

Correspondence should be addressed to Valentina Gargiulo; gargiulo@irc.cnr.it

Received 21 May 2019; Revised 11 August 2019; Accepted 5 September 2019; Published 29 September 2019

Academic Editor: Claudia Crestini

In this study, we highlighted how the catalytic effect of alkali metals on xylan pyrolysis is strongly affected by the adopted doping approach. Thermogravimetric and pyrolysis tests, up to 973 K and at a heating rate of 7 K/min, were conducted on a set of potassium- or sodium-doped xylan samples containing controlled amounts of KCl or NaCl introduced, starting from a demineralized xylan sample, through a conventional wet impregnation approach. Pyrolysis product yields from xylan-doped samples were compared with those related to the demineralized xylan sample. The performances of the doping procedure were assessed through a comparison with the data collected on raw xylan and a xylan sample doped with potassium ions by a cationic exchange approach. The results showed that the introduction of potassium ions by wet impregnation using a chloride salt negligibly affected the pyrolytic behaviour of the demineralized sample and indicated that the doping approach based on wet impregnation using chloride salts is not appropriate for the study of the effect of alkali metals on the pyrolysis of polysaccharides bearing acidic functional groups as xylan.

1. Introduction

The biomass pyrolysis is receiving increased interest from the scientific community since it is recognized as one of the most promising thermochemical conversion technologies able to convert biomass to value-added chemicals and fuels either in solid, liquid, and gas states. Moreover, being the plant matter used in this process produced by the photosynthetic reduction of carbon dioxide, the use of biomass-derived fuels can essentially be carbon neutral with respect to fossil fuels and the biomass can be considered a renewable energy source. The residual biomass valorisation in thermochemical conversion processes faces also the need of a correct disposal of vegetal residues and wastes [1].

In pyrolytic processes, the biomass is heated to moderate temperatures, 675–875 K, in the absence or with a very low amount of oxygen to produce solid, liquid, and gaseous products. Depending on the operating conditions, the pyrolysis processes can be divided into different subclasses: slow pyrolysis, conventional pyrolysis, fast pyrolysis, and flash pyrolysis. Slow pyrolysis is a process in which the heating rate is kept slow (approximately 0.1–10 K/s) leading to higher char yields at the expense of liquid and gaseous products. Fast pyrolysis is characterized by faster heating rates (about 10–200 K/s) and, among the different pyrolysis processes, it is considered the best one for producing liquids or gases. Flash pyrolysis is an alternative version of fast pyrolysis, in which the heating rates are very high, >1000 K/s, with reaction times of few to several seconds. These process conditions allow to produce high amounts of liquid products [2–5].

Products yields and compositions are proven to be strongly affected by the relative content of organic and inorganic biomass components [6–9]. A lot of research works have been focused on the study of biomass single components' (cellulose, hemicellulose, and lignin) pyrolysis behaviours, but how the inorganic compounds presence affects the pyrolysis of each biomass component is far to be fully understood and deserves further experimental studies.

A wide literature is available on the effect of AAEMs on the pyrolysis of biomasses and cellulose [10–17], whereas only few works reported about the effect of metals on hemicellulose pyrolysis [18–22]. Inherent alkali and alkaline earth metallic (AAEM) species are known to affect both the temperature and the mechanism of biomass thermal decomposition [23–25]. It has been proven that all the AAEMs promoted the ring scission and dehydration reactions in competition with the depolymerization, single dehydration, and water addition reactions whatever feedstocks are used, individual constituent or biomass samples [23–25]. However, K, Na, Ca, and Mg affect the primary decomposition of the organic constituents of the biomass at a different extent. Patwardhan et al. [12, 18] found that earth alkali metals were more effective in enhancing the formation of 2-furaldehyde and char at the expense of the other dehydration reaction products during the pyrolysis of both cellulose and hemicellulose. In particular, Patwardhan et al. [12] found that earth alkali metals significantly reduced the decomposition temperature of cellulose, and contrary to the alkali metals, their effect was found to be very dependent on the amount of loading below a certain limit [12].

Eom et al. established that potassium has a stronger catalytic effect on the ring scission reactions favouring char production and suppressing levoglucosan formation [11]. Also the production of C_6 lignin derivatives including phenol, guaiacol, and syringol seems to be promoted by the presence of this alkali metal [11].

In some cases, the effect of counterion was also assessed showing a clear effect of Cl^- in decreasing the levoglucosan yield favouring the production of furanic derivatives [12].

Compared to cellulose, hemicellulose pyrolysis was less studied because of its chemical heterogeneity, complexity, and less defined structure [26]. Moreover, the unsatisfactory isolation techniques concur to explain the very limited information about hemicellulose pyrolysis. These limitations lead to the choice of proxy compounds that are not representative of the whole spectrum of hemicelluloses actually present in the biomasses.

Depending on the type of plant source, hemicelluloses are classified as xylans (β-1,4-linked D-xylose units), xyloglucans (β-1,4-linked D-glucose units decorated with α-D-xylose units), mannans (β-1,4-linked D-mannose units), glucomannans (β-1,4-linked D-mannose and D-glucose units), and β-(1 $\longrightarrow$ 3, 1 $\longrightarrow$ 4)-glucans [26]. Xylans are the main hemicelluloses in hardwood. In almost all cases, the xylan backbone is substituted to varying degrees with monosaccharide or disaccharide side chains: glucuronic acid and 4-O-methyl glucuronic acid in glucuronoxylan, arabinose in arabinoxylan, and a combination of acidic and neutral sugars in glucuronoarabinoxylan [26].

Among the different polysaccharides usually used as hemicellulose model compounds, xylan and in particular glucuronoxylan are the most studied due to their abundance in hardwoods [26]. Glucuronoxylan is the major component of the secondary cell walls of dicots (15–30%), and it contains 4-O-methyl-GlcA residues attached to C-2 every 10 xylose residues; moreover, 70% of xylose units contain one O-acetyl group at C-2 or C-3 [26].

As in the case of cellulose, the pyrolysis of xylan-based hemicellulose yields both condensable and noncondensable products, as well as char [18, 20, 27–32]. Xylan-based hemicellulose is less stable than cellulose, so its thermal degradation occurs in a lower temperature range (493 to 588 K). Although both polysaccharides generate similar volatile products, including anhydrosugars, aldehydes, ketones, acids, and noncondensable gases (CO, CO_2, H_2, and light hydrocarbons up to three carbon units, C_3), xylan-based hemicellulose produces furan derivatives (2-furaldehyde the most abundant) in greater yields with respect to anhydrosugars [18, 28–30].

The few works available in the open literature suggest that xylan-based hemicellulose could exhibit competing pyrolysis pathways involving depolymerization and dehydration reactions to form furan and pyran ring derivatives. An alternative decomposition mechanism was postulated based on furanose and pyranose ring-breakage to form light oxygenated species and permanent gases via dehydration, enol-keto tautomerization and retro aldol reactions, or 2-furaldehyde via cyclization and dehydration reactions [18, 28–30].

Most of the experimental studies on the hemicellulose pyrolysis employ extracted or commercial xylan-based hemicellulose and overlook the effects of structural modifications (for example, the removal of acetyl groups) and the presence of metals (mostly AAEMs) sourced from hemicellulose isolation techniques. How the presence of inherent inorganics affects the pyrolytic decomposition pathways of hemicellulose is still an open question, and it deserves a great research effort to be completely understood.

Patwardan et al. [18] observed that, under fast pyrolysis conditions, some mineral species promote the ring scission to produce noncondensable gases and light oxygenated molecules and dehydration reactions to produce 2-furaldehyde and char in competition with depolymerization, water addition, and single dehydration reactions to produce xylose and anhydrosugars, respectively [18]. Experiments on beechwood xylan under slow pyrolysis conditions confirmed the role of AAEMs in favouring both char and gas productions but highlighted that dehydration reactions are depressed, while reactions leading to the formation of light oxygenates via ring scission are preferred [20]. Moreover, recent works on xylan doped through a cationic exchange approach with controlled quantities of potassium or sodium ions after a complete demineralization [21, 22] indicated that both K^+ and Na^+ favoured ring opening, rearrangement, and rehydration reactions leading to the production of low-molecular-weight compounds [21, 22]. The same authors highlighted, indeed, that the production of CO_2 is enhanced to a larger extent and its production in presence of metal ions is shifted at lower temperature confirming that the effect of alkali ions on ring scission reactions becomes more relevant with the increase in the ion concentration [21, 22].

The comprehension of the effects of minerals on xylan pyrolysis is also complicated by the presence in the xylan structure of carboxylic acids such as 4-O-MeGlcA, whose form (uronate vs. uronic acid form) alters the thermal behaviour of the polysaccharide [32].

In spite of huge efforts in this field, a comprehensive study about the influence of the different approaches to dope xylan with AAEMs has not been yet proposed. The simplest approach to dope biomass and biomass components is the wet impregnation [10–17]. This approach is based on a weak interaction between AAEMs and the feedstock and it works quite well with biomasses, lignin, and neutral polysaccharides as cellulose [10–17]. The results are not so obvious for polysaccharides bearing acidic functionalities as xylan, considered as representative of hemicellulose, since a tight interaction between AAEMs and the acidic moieties in the polysaccharides (uronates in the case of xylan) seems required [21, 22, 32].

In this work, the effect of AAEMs on hemicellulose pyrolysis was studied by doping through wet impregnation with different amounts of KCl or NaCl, a xylan polysaccharide free of metal contaminants. The pyrolytic behaviours of the correspondent doped samples were assessed by both thermogravimetric analyses and slow pyrolysis tests and compared with that of the demineralized sample chosen as benchmark. Chloride salts have been selected for wet impregnation since most of the experimental works dealing with the effect of AAEMs on the pyrolysis of cellulose and biomasses used samples impregnated with an aqueous solution of these salts [12, 13, 16, 17, 33, 34]. Since hemicellulose is a carbohydrate polymer as cellulose, alkali chlorides were used in this study with the aim of highlighting possible similarities between the pyrolytic behaviours of these two biomass components.

As the final goal, the appropriateness of wet impregnation, as typical doping procedure to obtain AAEM-doped xylan, was thoroughly investigated by comparing the results with the data collected on commercial xylan and a xylan sample doped with potassium ions by a cationic exchange approach [21].

2. Materials and Methods

2.1. Sample Preparation. All the chemicals used in this study were purchased from Sigma-Aldrich and used as received. Beechwood xylan (X4252) was used as pentose model compound of hardwood hemicellulose.

Raw xylan (X) was demineralized by means of a cationic exchange resin according to the procedure reported in [20]. In brief, 20 g of raw xylan was dissolved in 300 mL of water through sonication (10 min) and afterward vigorous stirring (1 h) obtaining a homogenous solution. The xylan solution passed through 20 mL of cationic exchange resin (Dowex® 50WX8; 100–200 mesh) in the H^+ form, and the resulting eluate (pH ~2.5) was freeze-dried and the demineralized sample (DX) was recovered as a light beige powder. The content of inorganics decreases from 4.4 wt.% in the raw xylan up to 0.6 wt.% in the demineralized sample (DX) [20]. The content of the main inorganics in raw and demineralized samples (data already reported by Giudicianni et al. [20]) is reported as Table S1 in the Supplementary Material section.

Doped samples were prepared according to the wet impregnation procedure as follows: 5 g of demineralized xylan was mixed with the appropriate amount of KCl dissolved in deionized water, and the resulting mixture was stirred for 30 min at ambient temperature to obtain a homogenous slurry and then dried in air at 50°C for 24 hours. Four KCl-doped samples (DX_$K_{wet(x)}$) containing 0.3, 0.5, 1.0, and 1.5 wt.% of K^+ (0.5, 1, 2, and 3 wt.% of KCl) were produced by dissolving each sample with 5 g of xylan and 0.025, 0.05, 0.1, and 0.15 g of KCl, respectively, in 50 mL of H_2O. With the same approach, a xylan-doped sample containing 1.1 wt.% of Na^+ (3 wt.% of NaCl) was also prepared by using 0.15 g of NaCl and named DX_$Na_{wet(1.1)}$.

The doped sample DX_$K_{resin(1.2)}$ was prepared according to procedure with the cationic exchange resin in the K^+ form, as reported in [21]. In brief, the cation exchange resin in the K^+ form was prepared by washing the Dowex resin (H^+ form) with a KOH 1 M solution until the eluate resulted basic. 5 g of DX was dissolved in 100 mL of distilled water, as previously described, and passed through 10 mL of resin in the K^+ form. The corresponding eluate was then dried in an oven at 50°C.

2.2. Characterization Methods. The thermal behaviour of the xylan-based samples was studied in a thermogravimetric (TG) apparatus (Pyris 1, PerkinElmer) by heating each sample (2–10 mg) from 323 K up to 973 K, at atmospheric pressure under an inert environment (N_2, 40 mL/min, heating rate 7 K/min).

Infrared spectroscopy (FTIR) analysis of the xylan-based samples was performed on pellets (13 mm diameter) obtained upon compression (10 ton for 10 minutes) of powdered dispersions prepared by mixing and grinding the samples (1–3 wt.%) with KBr. FTIR spectra in the 3600–400 cm^{-1} range were acquired in the transmission mode using a 5700 Nicolet spectrophotometer.

2.3. Pyrolysis Tests. Xylan-based samples were pyrolysed at 7 K/min up to 973 K in a lab-scale reactor described in detail elsewhere [8, 16, 17, 20–22]. The reactor consists in a prismatic jacketed chamber ($L = 0.024$ m, $W = 0.04$ m, and $H = 0.052$ m) into which 4 sample trays are allocated uniformly along the rectangular cross section of the inner reaction chamber and where the feedstock (4 g, 400–600 μm size range, predried at 378 K for 2 hours) is loaded in thin layers (toward 1 mm thick). The carrier gas (nitrogen) is heated at the programmed temperature via a PID controller by a superheater placed before the jacketed reactor and flows into the jacket at a constant gas mass flow rate (3.09 NL/min). The flow is then reversed toward the pyrolysis chamber and passes through a ceramic flow straightener before reentering the chamber. The residence time of the gas in the reaction chamber (2 s) is low enough to limit the secondary reactions of the volatiles evolving from the primary decomposition of the feedstock. N-type thermocouples monitor the temperature along the main dimension of the rectangular sample trays. Pressure transducers monitor the pressure along the carrier gas supply line and at both the inlet and outlet of the test chamber.

Condensable products (hereinafter "liquid products" or, briefly, "liquids") exiting the reactor flow through a closed

loop forced liquid cooling (water at 290 K was used as the cooling medium) and are collected in a flask submerged in a liquid argon trap (at 87 K). Noncondensable gases are sampled before the argon liquid trap and on-line analysed, after passing through different traps to remove the residual moisture, by a gas chromatograph equipped with a thermal conductivity detector (Agilent 3000 Quad). Temporal profiles of the release rates of CO, CO_2, H_2, CH_4, C_2H_4, and C_2H_6 evolving from the pyrolysis tests are obtained by continuously measuring the carrier gas flow rate and by determining the produced gas composition every 171.5 s.

The yields of the gaseous products are calculated by integrating the measured releasing rate curves along the test duration. The solid product (char) yield is determined gravimetrically, with respect to the fed sample, using a laboratory balance with 0.01 mg resolution. The liquids' yield is evaluated as the amount needed to close the mass balance.

The experiments were repeated twice. The relative difference between the measured and the average values of char, gas, and liquid yields was always lower than 5% of the measured values.

3. Results and Discussion

In this section, at first, the results of TG and slow pyrolysis tests on samples containing growing KCl amounts prepared by wet impregnation were compared in order to investigate the role of the metal ion load. This approach follows the one previously used by some of the authors to investigate the effect of potassium doping by wet impregnation on cellulose pyrolysis [17]. The results disclosed in the first part of this section have been strengthened also taking into account the effect of the cation type. To this aim, the results of slow pyrolysis tests on xylan samples doped by wet impregnation with a similar amount of K^+ and Na^+ were compared. The second part of this section was dedicated to the comparison with literature data available on raw xylan and a potassium-doped xylan sample prepared by a cationic exchange approach [21, 22].

3.1. Thermogravimetric Results. In this work, TGA was performed to study the pyrolytic behaviour of demineralized xylan and KCl xylan-doped samples under the same conditions settled during the pyrolysis tests (nitrogen, HR = 7 K/min, and end temperature 973 K).

Figure 1 reports the TG and DTG profiles of the four K-doped samples along that of the demineralized xylan (DX).

DX decomposes with a main thermal event occurring at 517 K and a second one between 560 and 660 K. A solid residue of 25.5 wt.% (evaluated on dry basis) was collected at the end of the thermal treatment. It is worthy of note that this thermal behaviour differs from the one usually exhibited by the raw xylan (not demineralized) [8, 16, 20, 32, 35–37] characterized by two main thermal events peaked around 510 and 550 K, respectively. For the sake of completeness, the raw xylan pyrolytic behaviour (data already reported by Giudicianni et al. [22]) was also compared with the above data and the comparison reported in the Supplementary Material section as Figure S1.

The KCl-doped samples decompose following the same TG profile of DX; indeed in the corresponding DTG curves, a main peak centred at 515 K and a shoulder between 560 and 670 K were found in all the cases. Just a slight anticipation of the polysaccharide devolatilization temperature was detected for all the doped samples (the temperature of maximum decomposition rate spans between 515 and 500 K), while the weight loss rate slightly decreases with the increase in KCl load. Overall, the qualitative trends of the DTG curves of the doped samples were not affected by the introduction of the growing amounts of KCl, but the maximum of the weight loss rate curves was slightly reduced (Figure 1). It is worthy of note that differently from what was previously observed for cellulose [16, 17], just a slight anticipation of the xylan initial devolatilization can be observed (about 15 K).

In accordance with the increasing amount of KCl, the solid residue amount measured at 973 K grows moving from DX to DX_$K_{wet(1.0)}$ (25.5 wt.% for DX up to 29 wt.% for DX_$K_{wet(1.0)}$) resulting, in the case of highest KCl loading, comparable to that of raw xylan (29.7 wt.% [20]).

3.2. Pyrolysis Test Results. The pyrolysis products (liquids, gases, and char) of the four KCl-doped xylan samples have been quantified and compared with those of the demineralized xylan (DX) in Table 1. The char yields have been corrected taking into account that the amount of KCl, added as a dopant, is completely recovered into the solid residue.

The slow pyrolysis of DX led to the production of 54.1 wt.% of liquid products, of 25.1 wt.% of a solid product (char), and of 20.8 wt.% of gaseous products. By comparing these yields with those of the doped samples, few differences arise. Indeed, even at high KCl load (3 wt.%), the doping approach by wet impregnation did not produce noticeable changes in the product yields distribution compared to DX. In particular, the yields of liquid products are very similar to those of DX, while, surprisingly, those of the gas fraction tend to decrease with the increase in KCl load. As concerns the char yielding, a slight increase is detected.

The similarity between the pyrolytic behaviours of DX and the four doped samples was also proved by analysing the evolution of the gaseous species along the pyrolysis temperature (Figure 2). In the Supplementary Material section, the comparison between the evolutions of the gaseous species along the pyrolysis temperature of doped samples and raw xylan (data already reported by Giudicianni et al. [22]) is also reported (Figure S2). The yields of the different gases produced during the pyrolysis tests have been also quantified and reported in Table S2 in the supporting information section.

For all the samples, CO_2 and CO were the main gaseous species produced, even though the production of CO_2 was predominant with respect to CO. Both gases are known to evolve from the ring opening reactions and from the cleavage of the more active side chain groups in depolymerized sugar units or rearrangement products [18, 28, 29].

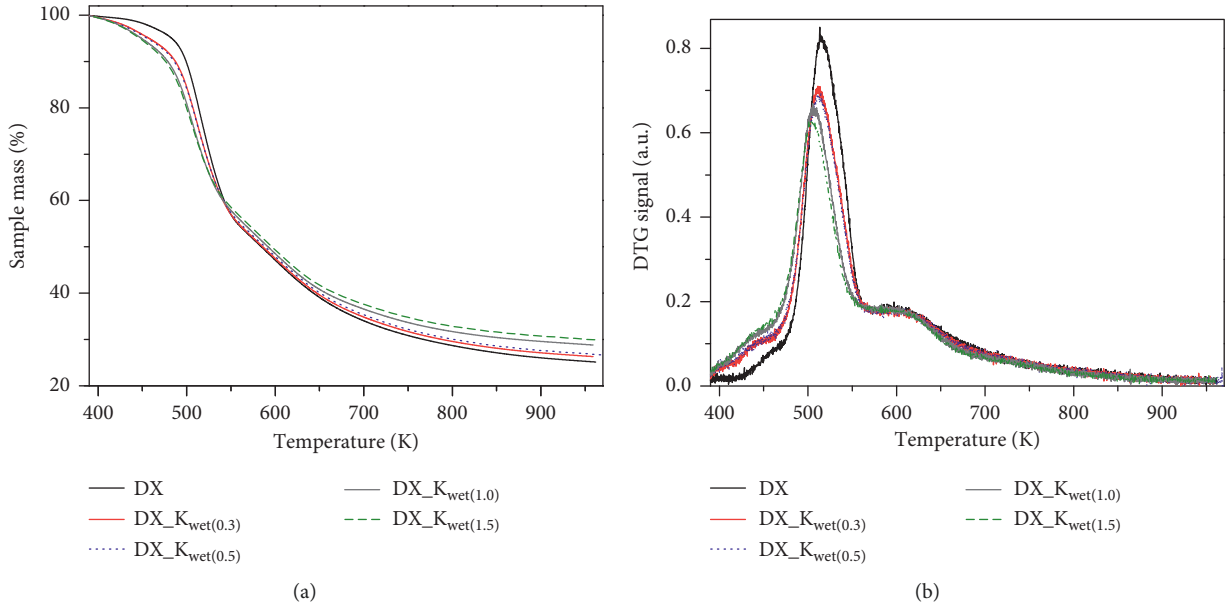

Figure 1: TG (a) and DTG (b) profiles of DX and the four xylan-doped samples (DX_K$_{wet}$).

Table 1: Pyrolysis product yields (dry basis) corrected taking into account the amount of dopant (KCl).

Samples	Char (wt.%)	Gas (wt.%)	Liquid (wt.%)
DX	25.1	20.8	54.1
DX_K$_{wet(0.3)}$	26.5	20.7	52.8
DX_K$_{wet(0.5)}$	27.8	20.4	51.8
DX_K$_{wet(1.0)}$	27.9	19.1	53.0
DX_K$_{wet(1.5)}$	26.9	19.3	53.8

In the case of DX, the CO_2 curve was characterized by two distinct events: the first one between 423 and 580 K and the second one in the 580–873 K temperature range, while the releasing curve of CO exhibited two overlapped events in the same temperature range of CO_2, but the first one is a shoulder on the increasing branch of the second main peak. The releasing curves of H_2 and CH_4, as expected, are located at higher temperature ranges since the production of both gases is related to secondary reactions [28].

The analysis of the releasing curves of CO_2, CO, H_2, and CH_4 of the four doped samples confirmed that the introduction of KCl by wet impregnation did not significantly affect the DX decomposition mechanism. It is worthy of noting only the slight enhancement of the first peak in both the CO_2 and CO releasing curves of all doped samples.

A pyrolysis test on a xylan sample doped with Na^+ (3 wt.% of NaCl and 1.1 wt.% of Na^+) by wet impregnation was further performed to confirm the limited suitability of the wet impregnation using chloride salts as a strategy to steer the pyrolytic pathways of xylan in presence of AAEMs (and, as a larger extent, of polysaccharides bearing acidic functional groups). In Figure 3, the comparison between the pyrolysis product yields of DX, DX_K$_{wet(1.0)}$, and DX_Na$_{wet(1.1)}$ is reported. The introduction of Na^+ by wet impregnation leads to results similar to those obtained with DX_K$_{wet(1.0)}$. This finding corroborates the thesis that neither the kind of cation nor the cation load have a significant effect on the pyrolytic behaviour of xylan when the wet impregnation with chloride salts is used as the doping approach.

It is worth of noting that the above disclosed results on the pyrolytic behaviour of xylan doped by wet impregnation differ from those obtained with cellulose fibres doped with K^+ up to 1.5 wt.% by following the same approach [17]. Such difference highlights the importance of taking into account the specific chemical nature of the polysaccharide in the selection of the most suitable doping approach: xylan is an acidic polysaccharide bearing carboxylate groups that forecast the establishing of an intimate contact with the doping cations (Na^+ or K^+) compared to weak electrostatic bonding establishing between cations and the neutral cellulose. The texture of the polysaccharide should be also taken into account since, differently from the nonfibrous hemicellulose, the cellulose fibres are porous matter that can be more efficiently and uniformly impregnated, leading to a better exploitation of the catalytic effect driven by the metal cations.

Finally, in the case of KCl- and NaCl- xylan-doped samples, the role of anionic counterion (Cl^-) acting as a slight inhibitor of the catalytic effect of potassium or sodium ions cannot be excluded. Patwardan et al. [12] recognized, in the case of fast pyrolysis of cellulose, a role of counteranion of the metal ions in the liquid products speciation, evidencing a clear effect of Cl^- in decreasing levoglucosan yield favouring the production of furanic derivatives (2-furaldeyde and 5-hydroxymethyl furfural) whose yields progressively increase with the increasing amount of Cl^-. In our recent work [22], we evidenced the effect of Na^+ doping (obtained by exploiting a cationic exchange resin approach) on xylan pyrolysis in modulating the yield of 2-furaldehyde

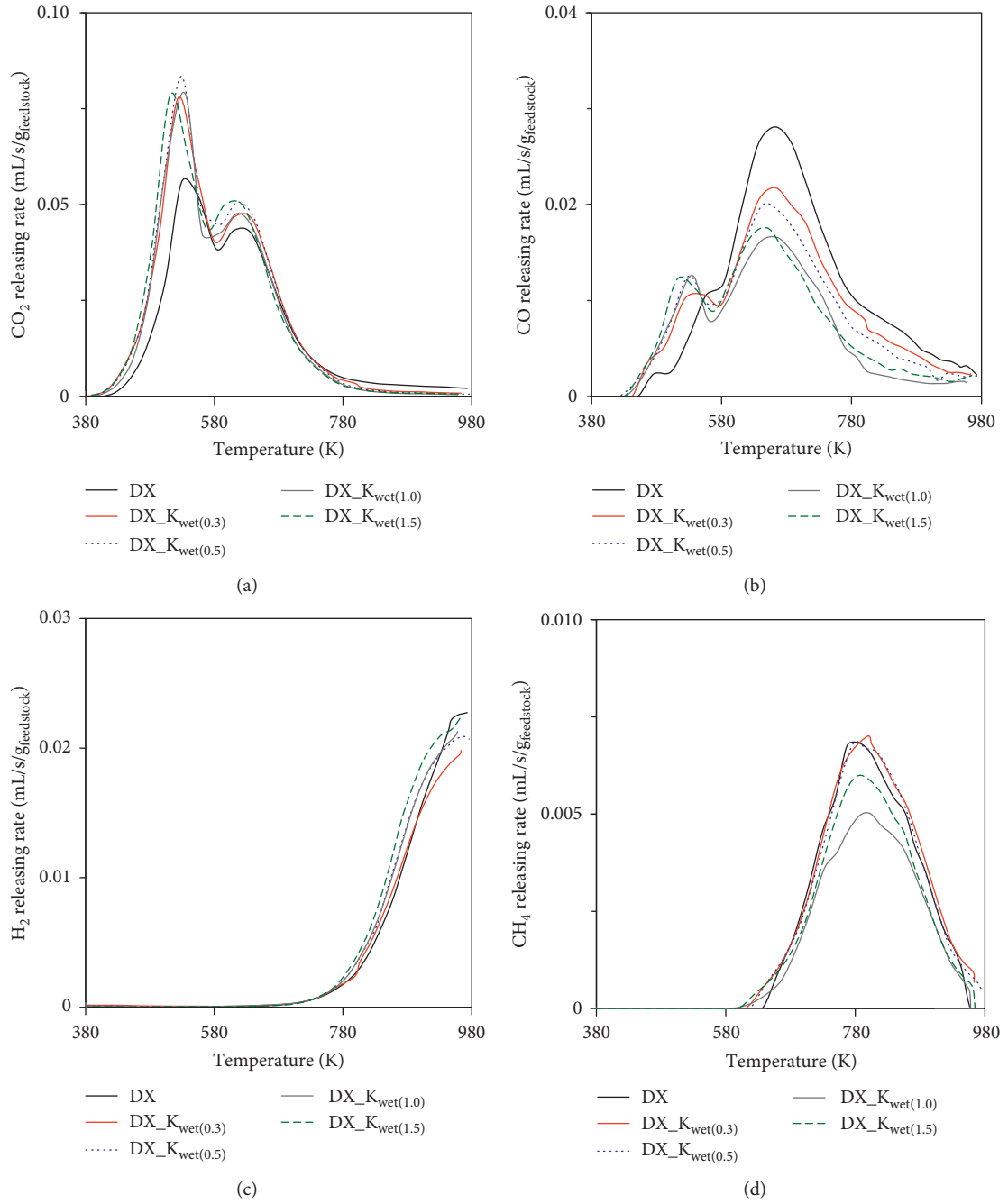

Figure 2: Gas releasing curves (CO_2, CO, H_2, and CH_4) of DX and DX_$K_{wet(x)}$ samples.

on the basis of Na^+ doping amount. In [22] the higher (but anyway lower when compared to the DX sample) liquid yield for the Na-doped xylan samples, in which the Cl^- counterion is absent, let us to speculate about a possible role also of chloride ions in orienting the pyrolytic pathways. Moreover, it cannot be excluded as an opposite effect between Na^+ (or K^+) and counterions (Cl^- or similar) in catalyzing the xylan pyrolysis. The effect of counterion so could not be neglected in the case of the wet impregnation approach, and this becomes truer considering counterions able to interact at a higher extent with xylan or its pyrolysis vapours (for example, carbonates [37]). The evaluation of the effect of counterions is beyond the scope of this work and surely it deserves more attention and a dedicated investigation.

3.3. Comprehensive Comparison between Wet Impregnation and Ion Exchange Doping Approaches. The importance of the strength of the interaction between the metal ion and the acidic polysaccharide (weak vs. tight interaction) and, as consequence, the effectiveness of the different doping approaches (wet impregnation using chloride salts vs. ion exchange) was further assessed by comparing the thermogravimetric and pyrolysis data of DX_$K_{wet(1.0)}$ and DX

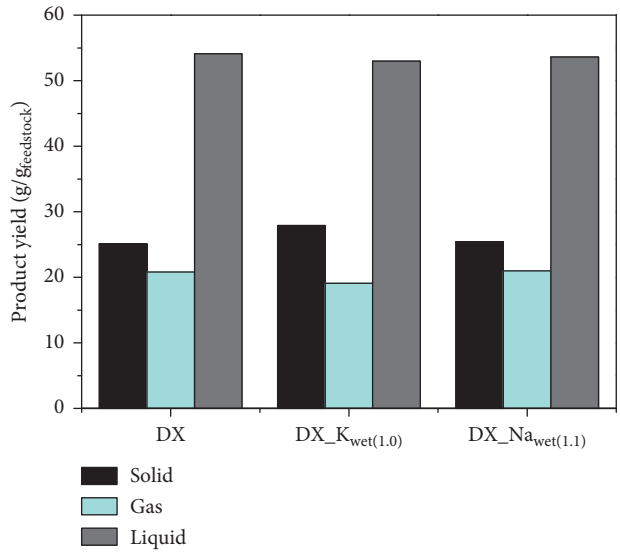

Figure 3: Pyrolysis product (solid, gas, and liquids) yields of DX and DX_K$_{wet(1.0)}$ and DX_Na$_{wet(1.1)}$.

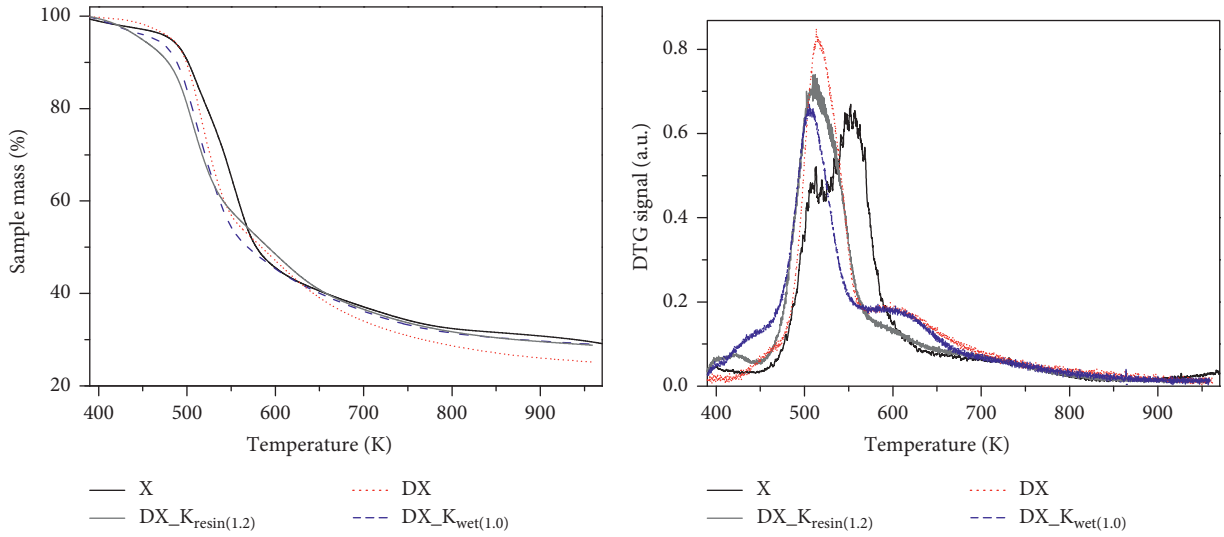

Figure 4: TG (a) and DTG (b) profiles of X DX, DX_K$_{wet(1)}$, and DX_K$_{resin(1.2)}$.

doped by using a cationic exchange approach [21], hereinafter DX_K$_{resin(1.2)}$, at comparable K^+ load (~1 wt.%). It was demonstrated that the pyrolytic behaviour of the cationic exchange-doped sample (DX_K$_{resin(1.2)}$) exhibited significant differences compared to those of DX and DX_K$_{wet(1.0)}$.

Figure 4 shows the TG profiles of DX_K$_{wet(1.0)}$ and DX_K$_{resin(1.2)}$ and the corresponding DTG curves. The data of X and DX were also reported for comparison being representative of AAEM-rich and AAEM-free samples [20], respectively.

The doped sample obtained by wet impregnation (DX_K$_{wet(1.0)}$) decomposes following the same TG profile of DX with a main event peaked at 517 K and a smaller event between 560 and 660 K. The same result is found for the sample doped by the cationic exchange approach (DX_K$_{resin(1.2)}$) except for the absence of the second event between 560 and 660 K. The behaviours of DX and of both doped samples are different from that of X, which is characterized by two thermal events peaked at 510 and 550 K, respectively. Recently, Wang et al. [32] suggested that the difference in the shape of raw and demineralized xylans TG curves can be explained by the influences of the chemical form of uronic acid residues (uronate or uronic forms) on the thermal reactivity of xylan during the heating process. In particular, 4-O-MeGlcA, when in the form of uronate, as in raw xylan, is supposed to be more thermally reactive and degraded before xylose units over the lower temperature range (below 500 K). On the opposite, 4-O-MeGlcA, when in the form of free carboxylic acid as in the demineralized

sample, decomposed simultaneously with the xylose units over a temperature range which is intermediate between the two degradation modes of the raw xylan [32] (between 470 and 570 K).

Figure 5 shows the yields of the pyrolysis products of DX, DX_$K_{wet(1.0)}$, and DX_$K_{resin(1.2)}$. X is also reported for comparison.

The data on the pyrolysis product distribution for the two doped samples are significantly contrasting: while KCl doping through wet impregnation did not produce noticeable changes in the product yield distribution compared to DX, the char and gas productions were promoted and that of liquid is depressed in DX_$K_{resin(1.2)}$. More in detail, the gas yield moves from 20.8 wt.% in DX up to 24.5 wt.% in DX_$K_{resin(1.2)}$, the liquid product yield decreases from 54.1 wt.% in DX up to 46.2 wt.% in DX_ $K_{resin(1.2)}$, and the char yield slightly increases passing from 25.1 wt.% in DX to 29.3 wt.% in DX_$K_{resin(1.2)}$. It is worthy to note that the product yields of the highly doped sample (DX_$K_{resin(1.2)}$) approach those obtained for the raw xylan sample (X) (Figure 5) [21].

Additional indications were achieved by comparing the evolution of the gaseous species during the pyrolysis process. The releasing rate curves of the main gaseous species (CO_2, CO, H_2, and CH_4) are shown in Figure 6. Since the yields of the different gases produced during the pyrolysis tests of X, DX, and DX_$K_{resin(1.2)}$ have been already reported by Gargiulo et al. [21], the comparison with those of DX_$K_{wet(1.0)}$ is reported as Table S3 in the Supplementary Material section.

The introduction of K^+ into the demineralized sample by wet impregnation using KCl, as stated before, did not induce great modifications on the decomposition mechanism of DX except for a slight enhancement of the first peak of CO_2 release rate. Conversely, the K^+ doping through cationic exchange resin induced significant modifications on the releasing rate of all the detected gaseous species (Figure 6) [21]. In particular, in both CO_2 and CO releasing rate curves, an enhancement of the first event in the 423–580 K temperature range was observed, whereas only for the CO releasing rate curve, the decrease of the second peak occurred. Moreover, in the case of H_2 and CH_4, an enhancement of the releasing rate curves is detected when the doping of the sample is performed by cationic exchange [21].

The enhanced production of permanent gases and in particular of CO_2 is ascribable to the catalytic effect of K^+ favouring ring opening, rearrangement, and rehydration reactions [28–30].

The effect of demineralization and the contrasting results between the two doping approaches can be interpreted again on the basis of different xylan thermal reactivities depending on the forms of 4-O-MeGlcA (uronate vs. neutral uronic acid) [32].

In X and DX_$K_{resin(1.2)}$, 4-O-MeGlcA units are expected to be in form of uronates, allowing a tighter interaction between the polysaccharidic chain and the cationic ions through ionic bonding (Na^+, K^+, and others in X and K^+ in DX_$K_{resin(1.2)}$) with the result of enhancing the catalytic effect of the metal ion (Figure 7).

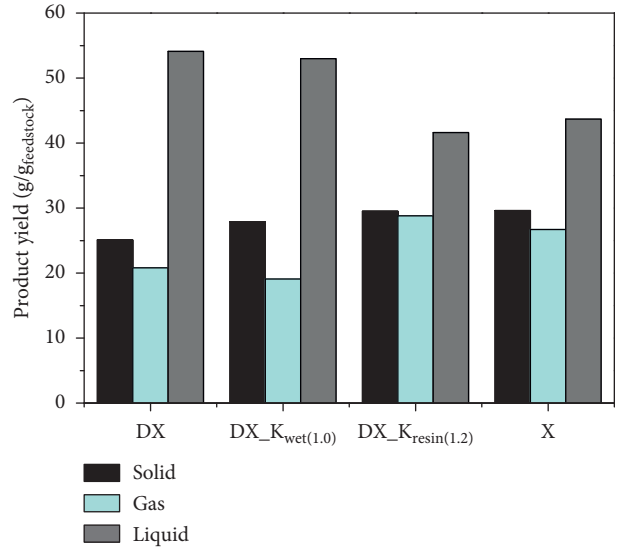

Figure 5: Yields of the pyrolysis products of X, DX, DX_$K_{wet(1.0)}$, and DX_$K_{resin(1.2)}$.

On the contrary, the wet impregnation procedure with KCl is expected to not allow the complete exchange between the H^+ and K^+ to transform the COOH group of glucuronic units into the COO^-K^+ form (Figure 7). Given this, a tight interaction between the glucuronic units in the xylan and the potassium ions cannot be established resulting in a lowering of the catalytic effect.

To confirm this aspect, a survey by FTIR spectroscopy was performed on DX, DX_$K_{wet(1.0)}$, DX_$K_{resin(1.2)}$, and X. In Figure 8, the four FTIR spectra, as well as an enlargement of the region between 1500 and 1900 cm^{-1} where the carboxylic and carboxylate stretching signals (at 1750 and 1600 cm^{-1}, respectively) occurred [38], are reported.

Through the comparison of the spectral features, it can be inferred that DX_$K_{resin(1.2)}$ is richer in carboxyl functional groups in the carboxylate form (uronate form) than DX_$K_{wet(1.0)}$ and that the spectroscopic shape of DX_$K_{resin(1.2)}$ resembles that of X rather than DX_$K_{wet(1.0)}$.

These spectroscopic findings confirm the expected differences between the uronate/uronic distributions in the investigated samples.

As a final remark, it has to be underlined that the above findings do not allow a fully understanding of the different thermal behaviours of the samples. Although a spectroscopic similarity between X and DX_$K_{resin(1.2)}$ and a good agreement between their pyrolytic behaviours (product yields and gas releasing curves) were found, the thermogravimetric data of the two samples are different (the two thermal events characteristic of X are not found also for DX_$K_{resin(1.2)}$). This means that other aspects (for example, the presence of monovalent and divalent cations in the commercial material (X)) have to be taken into account, and further studies to understand the reason of such differences are needed.

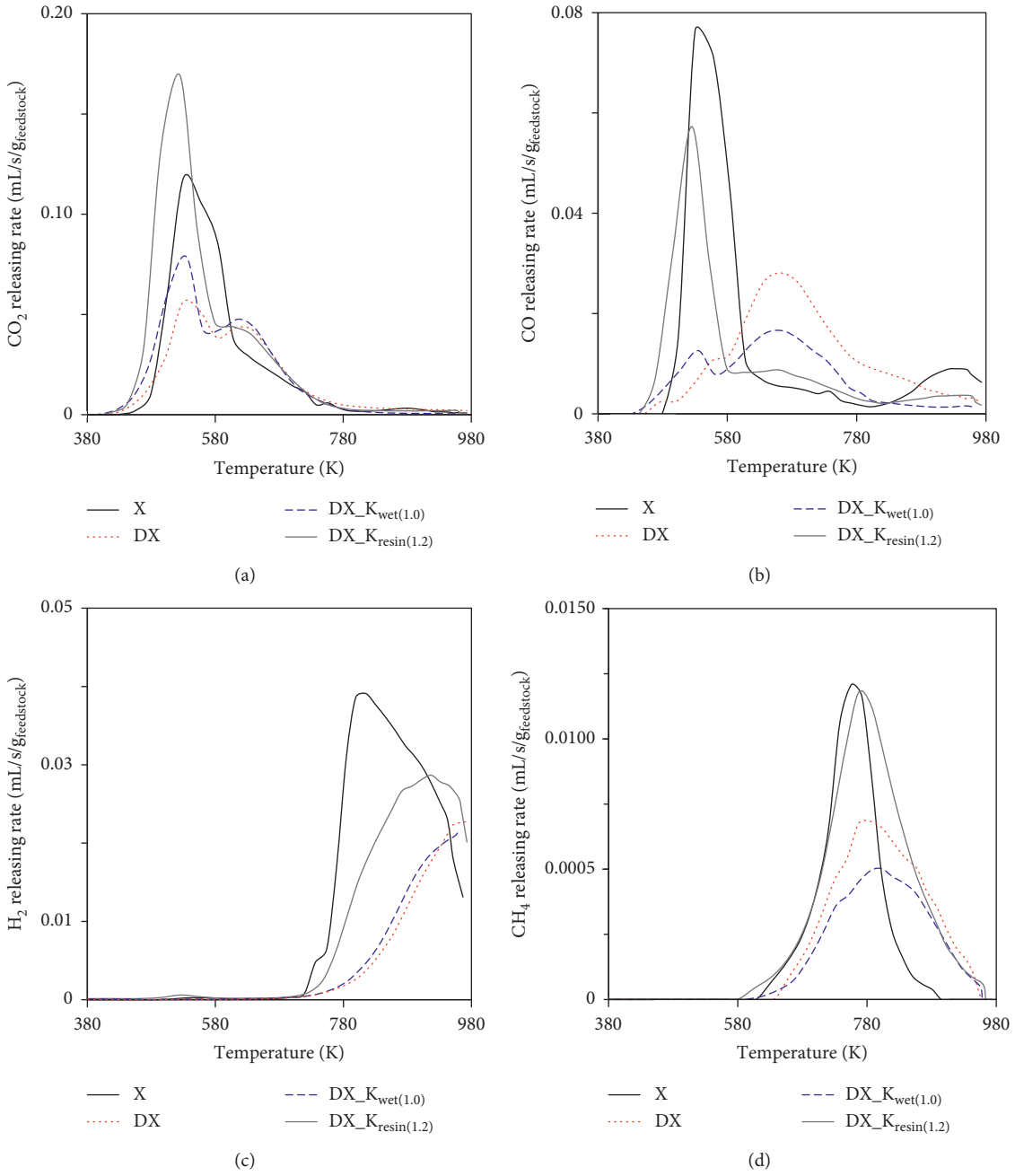

FIGURE 6: Releasing rate profiles along the temperature of the main gaseous species produced during X, DX, DX_$K_{wet(1.0)}$, and DX_$K_{resin(1.2)}$ pyrolysis.

4. Conclusions

In this work, the pyrolytic behaviour of different KCl xylan-doped samples was assessed by thermogravimetric analyses and slow pyrolysis tests (final temperature 973 K, heating rate 7 K/min). Xylan samples doped with increasing amounts of KCl were produced by wet impregnation and tested under slow pyrolysis conditions, and the corresponding results were compared with those obtained on a demineralized xylan sample. A comparison with a NaCl xylan-doped sample was performed to evaluate also the effect of the type of cation (K^+ and Na^+). A comparison with the results related to xylan-doped samples obtained by different doping approaches (cationic resin exchange) was finally carried out.

The collected results state the following:

(i) The introduction of metal ions in form of chloride salts through the classical wet impregnation has a negligible effect on the pyrolytic behaviour of an acidic polysaccharide as xylan.

(ii) Neither the kind of cation nor the cation load seems to affect the pyrolytic behaviour of xylan when the wet impregnation using chloride salts is used as the doping approach.

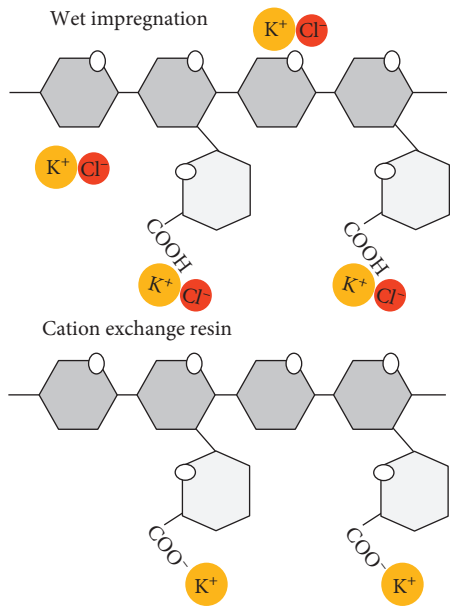

Figure 7: Scheme describing the results of wet impregnation and cation exchange doping procedures.

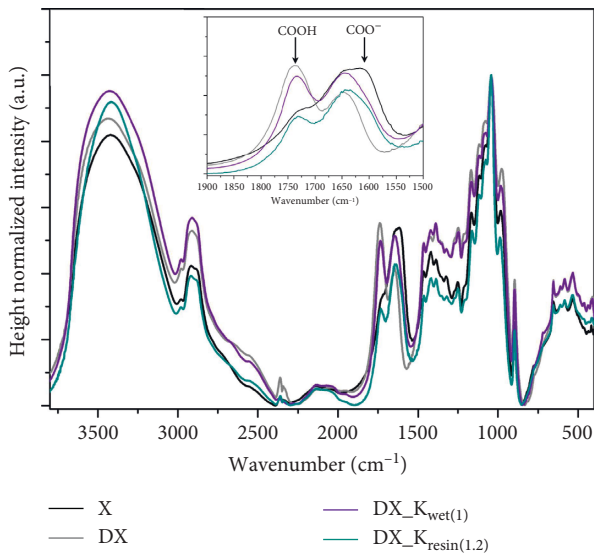

Figure 8: FTIR profiles of X, DX, DX_$K_{wet(1.0)}$, and DX_$K_{resin(1.2)}$.

(iii) In the case of wet impregnation, the detrimental effect of the counterion (Cl^-) in inhibiting the catalytic effect of AAEMs could not be excluded: given these circumstances, the role of the counterion in the wet impregnation doping procedure needs to be addressed.

(iv) The doping approach based on wet impregnation using chloride salts has a limited effectiveness compared to the cationic exchange approach since it does not assure a tight interaction between the polysaccharidic chain and the AAME ions through ionic bonding, mandatory for the exploitation of the catalytic effect.

(v) The doping through the cationic exchange approach simulates in a more realistic way the product yields and pyrolytic behaviour of a raw xylan, compared to the wet impregnation approach using chloride salts. This finding represents a great relevance result when approaching modelling of a real biomass where AAEMs are tightly bonded to the biomass components.

Data Availability

The data used to support the findings of this study are available from the corresponding author upon request.

Conflicts of Interest

The authors declare that this work was conducted in the absence of any commercial or financial relationships that could be construed as a potential conflict of interest.

Acknowledgments

The authors acknowledge Fernando Stanzione of IRC-CNR for ICP-MS analysis. The authors would like to acknowledge also the contribution of the COST Action CM1404 (Smartcats). This work has been carried out thanks to the financial support of the Accordo di Programma CNR-MSE 2013-2014 under the contracts "Miglioramento dell'efficienza energetica dei sistemi di conversione locale di energia" and "Bioenergia Efficiente" and the Accordo di Programma CNR-MSE 2016-2017 under the contract "MicroBio-CHP."

Supplementary Materials

The supplementary materials contain the detailed inorganic composition of raw and demineralized xylan samples (Table S1), the comparison among TGA results including also the raw xylan (Figure S1), the comparison among gas releasing curves including also the raw xylan (Figure S2), and the yields of main gaseous species (CO, CO_2, H_2, CH_4, C_2H_4, and C_2H_6) produced during pyrolysis tests (Tables S2 and S3). (*Supplementary Materials*)

References

[1] A. V. Bridgwater, "Renewable fuels and chemicals by thermal processing of biomass," *Chemical Engineering Journal*, vol. 91, no. 2-3, pp. 87–102, 2003.

[2] M.-K. Bahng, C. Mukarakate, D. J. Robichaud, and M. R. Nimlos, "Current technologies for analysis of biomass thermochemical processing: a review," *Analytica Chimica Acta*, vol. 651, no. 2, pp. 117–138, 2009.

[3] T. Bridgwater, "Biomass for energy," *Journal of the Science of Food and Agriculture*, vol. 86, no. 12, pp. 1755–1768, 2006.

[4] T. Kan, V. Strezov, and T. J. Evans, "Lignocellulosic biomass pyrolysis: a review of product properties and effects of pyrolysis parameters," *Renewable and Sustainable Energy Reviews*, vol. 57, pp. 1126–1140, 2016.

[5] M. Balat, M. Balat, E. Kırtay, and H. Balat, "Main routes for the thermo-conversion of biomass into fuels and chemicals.

Part 1: pyrolysis systems," *Energy Conversion and Management*, vol. 50, no. 12, pp. 3147–3157, 2009.

[6] Q. Liu, Z. Zhong, S. Wang, and Z. Luo, "Interactions of biomass components during pyrolysis: a TG-FTIR study," *Journal of Analytical and Applied Pyrolysis*, vol. 90, no. 2, pp. 213–218, 2011.

[7] S. Wang, X. Guo, K. Wang, and Z. Luo, "Influence of the interaction of components on the pyrolysis behavior of biomass," *Journal of Analytical and Applied Pyrolysis*, vol. 91, no. 1, pp. 183–189, 2011.

[8] P. Giudicianni, G. Cardone, and R. Ragucci, "Cellulose, hemicellulose and lignin slow steam pyrolysis: thermal decomposition of biomass components mixtures," *Journal of Analytical and Applied Pyrolysis*, vol. 100, pp. 213–222, 2013.

[9] S. Zhao, M. Liu, L. Zhao, and L. Zhu, "Influence of interactions among three biomass components on the pyrolysis behavior," *Industrial & Engineering Chemistry Research*, vol. 57, no. 15, pp. 5241–5249, 2018.

[10] F.-X. Collard, J. Blin, A. Bensakhria, and J. Valette, "Influence of impregnated metal on the pyrolysis conversion of biomass constituents," *Journal of Analytical and Applied Pyrolysis*, vol. 95, pp. 213–226, 2012.

[11] I.-Y. Eom, J.-Y. Kim, T.-S. Kim et al., "Effect of essential inorganic metals on primary thermal degradation of lignocellulosic biomass," *Bioresource Technology*, vol. 104, pp. 687–694, 2012.

[12] P. R. Patwardhan, J. A. Satrio, R. C. Brown, and B. H. Shanks, "Influence of inorganic salts on the primary pyrolysis products of cellulose," *Bioresource Technology*, vol. 101, no. 12, pp. 4646–4655, 2010.

[13] N. Shimada, H. Kawamoto, and S. Saka, "Different action of alkali/alkaline earth metal chlorides on cellulose pyrolysis," *Journal of Analytical and Applied Pyrolysis*, vol. 81, no. 1, pp. 80–87, 2008.

[14] H. Kawamoto, D. Yamamoto, and S. Saka, "Influence of neutral inorganic chlorides on primary and secondary char formation from cellulose," *Journal of Wood Science*, vol. 54, no. 3, pp. 242–246, 2008.

[15] S. M. Shaik, P. N. Sharratt, and R. B. H. Tan, "Influence of selected mineral acids and alkalis on cellulose pyrolysis pathways and anhydrosaccharide formation," *Journal of Analytical and Applied Pyrolysis*, vol. 104, pp. 234–242, 2013.

[16] V. Gargiulo, P. Giudicianni, M. Alfè, and R. Ragucci, "Influence of possible interactions between biomass organic components and alkali metal ions on steam assisted pyrolysis: a case study on *Arundo donax*," *Journal of Analytical and Applied Pyrolysis*, vol. 112, pp. 244–252, 2015.

[17] A. I. Ferreiro, M. Rabaçal, M. Costa, P. Giudicianni, C. M. Grottola, and R. Ragucci, "Modeling the impact of the presence of KCl on the slow pyrolysis of cellulose," *Fuel*, vol. 215, pp. 57–65, 2018.

[18] P. R. Patwardhan, R. C. Brown, and B. H. Shanks, "Product distribution from the fast pyrolysis of hemicellulose," *ChemSusChem*, vol. 4, no. 5, pp. 636–643, 2011.

[19] P. Rutkowski, "Pyrolysis of cellulose, xylan and lignin with the K_2CO_3 and $ZnCl_2$ addition for bio-oil production," *Fuel Processing Technology*, vol. 92, no. 3, pp. 517–522, 2011.

[20] P. Giudicianni, V. Gargiulo, C. M. Grottola, M. Alfè, and R. Ragucci, "Effect of alkali metal ions presence on the products of xylan steam assisted slow pyrolysis," *Fuel*, vol. 216, pp. 36–43, 2018.

[21] V. Gargiulo, P. Giudicianni, M. Alfè et al., "Experimental investigation on the effect of K^+ ions on the slow pyrolysis of xylan," *Chemical Engineering Transaction*, vol. 65, pp. 553–558, 2018.

[22] P. Giudicianni, V. Gargiulo, M. Alfè et al., "Slow pyrolysis of xylan as pentose model compound for hardwood hemicellulose: a study of the catalytic effect of Na ions," *Journal of Analytical and Applied Pyrolysis*, vol. 137, pp. 266–275, 2019.

[23] A. Saddawi, J. M. Jones, and A. Williams, "Influence of alkali metals on the kinetics of the thermal decomposition of biomass," *Fuel Processing Technology*, vol. 104, pp. 189–197, 2012.

[24] D. Mourant, Z. Wang, M. He et al., "Mallee wood fast pyrolysis: effects of alkali and alkaline earth metallic species on the yield and composition of bio-oil," *Fuel*, vol. 90, no. 9, pp. 2915–2922, 2011.

[25] R. Fahmi, A. V. Bridgwater, I. Donnison, N. Yates, and J. M. Jones, "The effect of lignin and inorganic species in biomass on pyrolysis oil yields, quality and stability," *Fuel*, vol. 87, no. 7, pp. 1230–1240, 2008.

[26] H. V. Scheller and P. Ulvskov, "Hemicelluloses," *Annual Review of Plant Biology*, vol. 61, no. 1, pp. 263–289, 2010.

[27] X. Zhou, W. Li, R. Mabon, and L. J. Broadbelt, "A critical review on hemicellulose pyrolysis," *Energy Technology*, vol. 5, no. 1, pp. 52–79, 2017.

[28] D. K. Shen, S. Gu, and A. V. Bridgwater, "Study on the pyrolytic behaviour of xylan-based hemicellulose using TG-FTIR and Py-GC-FTIR," *Journal of Analytical and Applied Pyrolysis*, vol. 87, no. 2, pp. 199–206, 2010.

[29] X. Zhou, W. Li, R. Mabon, and L. J. Broadbelt, "A mechanistic model of fast pyrolysis of hemicellulose," *Energy & Environmental Science*, vol. 11, no. 5, pp. 1240–1260, 2018.

[30] D. K. Shen, S. Gu, and A. V. Bridgwater, "The thermal performance of the polysaccharides extracted from hardwood: cellulose and hemicellulose," *Carbohydrate Polymers*, vol. 82, no. 1, pp. 39–45, 2010.

[31] K. Werner, L. Pommer, and M. Broström, "Thermal decomposition of hemicelluloses," *Journal of Analytical and Applied Pyrolysis*, vol. 110, pp. 130–137, 2014.

[32] J. Wang, M. Asmadi, and H. Kawamoto, "The effect of uronic acid moieties on xylan pyrolysis," *Journal of Analytical and Applied Pyrolysis*, vol. 136, pp. 215–221, 2018.

[33] S. Wang, Q. Liu, Y. Liao, Z. Luo, and K. Cen, "A study on the mechanism research on cellulose pyrolysis under catalysis of metallic salts," *Korean Journal of Chemical Engineering*, vol. 24, no. 2, pp. 336–340, 2007.

[34] A. Jensen, K. Dam-Johansen, M. A. Wójtowicz, and M. A. Serio, "TG-FTIR study of the influence of potassium chloride on wheat straw pyrolysis," *Energy & Fuels*, vol. 12, no. 5, pp. 929–938, 1998.

[35] S. D. Stefanidis, K. G. Kalogiannis, E. F. Iliopoulou, C. M. Michailof, P. A. Pilavachi, and A. A. Lappas, "A study of lignocellulosic biomass pyrolysis via the pyrolysis of cellulose, hemicellulose and lignin," *Journal of Analytical and Applied Pyrolysis*, vol. 105, pp. 143–150, 2014.

[36] H. Zhou, Y. Long, A. Meng, S. Chen, Q. Li, and Y. Zhang, "A novel method for kinetics analysis of pyrolysis of hemicellulose, cellulose, and lignin in TGA and macro-TGA," *RSC Advances*, vol. 5, no. 34, pp. 26509–26516, 2015.

[37] S. Zhao, M. Liu, L. Zhao, and J. Lu, "Effects of organic and inorganic metal salts on thermogravimetric pyrolysis of biomass components," *Korean Journal of Chemical Engineering*, vol. 34, no. 12, pp. 3077–3084, 2017.

[38] R. M. Silverstein, F. X. Webster, and D. J. Kiemle, *Spectrometric Identification of Organic Compounds*, Wiley, New York, NY, USA, 7th edition, 2005.